

An Electrostatic Model of Split-Gate Quantum Wires

Yinlong Sun and George Kirczenow

Department of Physics, Simon Fraser University

Burnaby, British Columbia, Canada V5A 1S6

Andrew. S. Sachrajda and Yan Feng

Institute of Microstructural Sciences, National Research Council

Ottawa, Ontario, Canada K1A 0R6

(Received December 12, 1994)

We present a theoretical model of split-gate quantum wires that are fabricated from GaAs-AlGaAs heterostructures. The model is built on the physical properties of donors and of semiconductor surfaces, and considerations of equilibrium in such systems. Based on the features of this model, we have studied different ionization regimes of quantum wires, provided a method to evaluate the shallow donor density, and calculated the depletion and pinchoff voltages of quantum wires both before and after illumination. A real split-gate quantum wire has been taken as an example for the calculations, and the results calculated for it agree well with experimental measurements. This paper provides an analytic approach for obtaining much useful information about quantum wires, as well as a general theoretical tool for other gated nanostructure systems.

PACS number: 73. 20. Dx

I. INTRODUCTION

Modern material-growing techniques such as molecular beam epitaxy and organo-metallic chemical vapour deposition make it possible to fabricate extremely clean semiconductor heterostructures. [1] In a modulation-doped [2] GaAs-Al_xGa_{1-x}As heterostructure, a two-dimensional electron gas (2DEG) is present at the interface of Al_xGa_{1-x}As and GaAs layers. [3] This 2DEG can be further confined laterally by various confining techniques such as electron-beam lithography [4], ion-beam exposure [5–7], or etching [8–10], forming a quasi-one-dimensional system usually called a quantum wire. At present, one widely used confinement method is the split-gate technique [11,12]. In a split-gate quantum wire, when a sufficiently negative voltage is applied to the metallic gates, electrons are completely depleted from under the gates, leaving a central channel of electrons undepleted. By further increasing the gate voltage negatively, the density of electrons in the channel is decreased continuously until the channel pinches off. Such quantum wires display unique fascinating properties which have stimulated many theoretical and experimental studies of their physics. [13] Because of the sophisticated gating technique and the flexibility of changing the density of electrons by varying the gate voltage, the split-gate quantum wires hold a great potential for realistic applications [14,15].

Considerable progress has been made in developing an understanding of the electronic structure of quantum wires theoretically, based on the results of computer simulations and analytic work. [16–23] However, for many systems, particularly those with an exposed semiconductor surface between the split metallic gates, the current understanding is not complete. For example, it has not been possible to predict accurately the pinchoff voltage of a quantum wire, given the knowledge of the geometric and doping parameters and the history of a given sample. The pinchoff voltage is the gate voltage at which conduction through the wire ceases. It is a quantity of considerable practical importance for these devices.

In this paper, we present a study that addresses such issues. In Section II A we describe the basic physical features of gated quantum wires that are included in our model. In

Sections II B and II C we point out that three qualitatively different ionization regimes can exist in the doped layer that supplies electrons to the quantum wire, and show how the ionization regime that a particular sample is in can be identified. We also show how the shallow donor density in the doped layer may be calculated. In Section II D we describe the calculation within our model of the depletion voltage for the electron gas under the gates. In Section II E we calculate the pinchoff voltage of the quantum wire. This calculation uses a Green's function method, which is an extension of the previous theoretical work of Davies [19] but treats the effects of the charges at the exposed semiconductor surface more accurately. In Section III, we take a well-characterized real sample as an example for calculations, and find good quantitative agreement between the calculated and measured depletion and pinchoff voltages both before and after illumination.

II. MODEL AND FORMALISM

We consider an infinitely long split-gate quantum wire whose crosssection is shown in FIG. 1. The layers from top are the GaAs cap, the Si-doped $\text{Al}_x\text{Ga}_{1-x}\text{As}$, the undoped $\text{Al}_x\text{Ga}_{1-x}\text{As}$ spacer, and the GaAs channel; their thicknesses are l_c , l_d , l_s , and l_{ch} , respectively. On top of the GaAs cap are two metallic gates with a spatial separation $2w$. The coordinate frame is chosen in such a way that the exposed surface of GaAs cap is the $z = 0$ plane, and the lateral direction is along the x-axis.

In such quantum wires, electrons donated by the Si donors in the doped $\text{Al}_x\text{Ga}_{1-x}\text{As}$ layer transfer to the $z = 0$ plane to fill the surface or interface states, and to the $z = L = l_c + l_d + l_s$ plane to form the 2DEG. This transfer of electrons leaves a positive spatial charge in the doped layer and thus causes the conduction band to bend within the heterostructure. One possible case of the band bending is shown in FIG. 2. The curve depicts to the bottom of the conduction band along the z-axis. Within the cap and the spacer layers, the curve is linear because there is no spatial charge in these layers. In the doped layer, however, the bottom of the conduction band is curved because of the presence of the spatial charge. The curve is

parabolic if the spatial charge density is uniform. E_{off} is the conduction band offset which occurs at the two interfaces between the GaAs and $\text{Al}_x\text{Ga}_{1-x}\text{As}$ layers. The whole system shown is in equilibrium, that is, the system has a uniform Fermi energy. (This may change when a voltage is applied between the gates and 2DEG, as is discussed below.) Note that, in the situation shown in FIG. 2, there is an unionized region in the doped layer where the conduction band is flat because donors are not ionized there. A detailed discussion of the features of our model now follows.

A. Model Description

Our theoretical model of split-gate quantum wires has four key features.

Feature 1) The Si donors are uniformly distributed in the $\text{Al}_x\text{Ga}_{1-x}\text{As}$ doped layer and divided into two categories: the shallow levels and the deep levels. We assume that electrons are donated only by the ionized shallow donors whose bound energy levels are above the Fermi level. Deep donors can be ionized by illumination.

It is well-known that the electronic state associated with a shallow donor in $\text{Al}_x\text{Ga}_{1-x}\text{As}$ has the hydrogenic form and can be handled with the effective mass theory [24]. Neglecting central cell effects, the binding energy of a shallow donor is $E_s = m^*e^4/2(4\pi\epsilon\epsilon_0\hbar)^2 = m^*/\epsilon^2(\text{Ryd})$, where m^* is the effective mass of the electron and ϵ is the dielectric constant. In $\text{Al}_x\text{Ga}_{1-x}\text{As}$, the Γ valley of the conduction band is the lowest one when $x < 0.45$. In quantum wires, x is usually in this regime. At the minimum point of the Γ valley, $m^* = 0.067 m_e$ and $E_s \approx 6 \text{ meV}$ correspondingly. Such a binding energy of shallow donors has been verified by various measurements [25,26]. Because E_s is much less than other relevant parameters such as the Schottky barrier and the conduction band offset, we consider E_s to be negligible small.

In the doped $\text{Al}_x\text{Ga}_{1-x}\text{As}$ layer, when $x > 0.2$, the ground state of a Si donor is the deep level instead of the shallow level. [27] It is now generally accepted that the deep level is

associated with a local lattice distortion which is usually called a DX center [28,29]. During illumination, a deep donor may absorb a photon and thus ionize. At low temperatures, however, a shallow donor can not change into a deep donor automatically because of the energy barrier associated with the lattice distortion. This argument is supported by many studies such as persistent-photoconductivity experiments [30].

Accordingly, we have

$$N_{total} = N_s + N_d, \quad (1)$$

where N_{total} , N_s , and N_d are the total, shallow, and deep donor concentrations, respectively. For a quantum wire, N_{total} can be obtained from the fabrication parameters but N_s and N_d are undetermined experimentally. This has made it difficult to analyze quantum wires theoretically because N_s determines the number of donated electrons and the spatial charge density. However, we will describe a method to calculate N_s within our model.

Feature 2) The Schottky barrier between the metallic gates and the GaAs cap is determined by the type of the gate metal and the type of GaAs interface, and is independent of the gate voltage. The surface states of the exposed GaAs surface are pinned at a single energy level within the forbidden band gap of GaAs. The surface states are localized and surface electrons have a low mobility.

The Schottky barrier of a metal-semiconductor contact refers to the energy difference between the conduction band minima of the semiconductor at the interface and the Fermi level of electrons in the metal. It is generally believed [31] that Schottky barriers are associated with the metal-induced gap states which depend only on the type of the contact metal and the type of the semiconductor interface. This means that, in quantum wires, the Schottky barrier between the gates and the GaAs cap is independent of the gate voltage. For (100) and (110) interfaces of GaAs, the Schottky barriers for many metals have been measured [32–34].

The surface states of GaAs are associated with the dangling bonds at the exposed surface. The physics of surface states is complicated and there has been no generally accepted model

yet. [31] However, experiments show that the surface states of GaAs are pinned at a single energy value within the forbidden band gap as long as the surface is covered by a fraction of an adatom monolayer. [35] For example, the surface states of the n-type GaAs (100) surface are pinned at about 0.8 eV below the bulk conduction band minima. [36] Some calculations [37,38] also show that the surface states are very localized, which means that the surface electrons have a very low mobility.

The Schottky barrier of the exposed surface refers to the energy difference between the conduction band minima and the pinned surface level (see FIG. 2). In the following discussion, we use Φ_{sb} for the Schottky barrier of the exposed surface and Φ'_{sb} for the Schottky barrier of the metal-GaAs contact.

Feature 3) The energy barrier due to the spacer layer is small. Therefore we assume that the electrons on either sides of it are always in equilibrium with each other. The energy barrier that separates the surface electrons is so high that tunneling of electrons through it can be neglected. Therefore we assume that the total number of surface electrons is conserved when the gate voltage varies.

This feature can be justified by that the tunneling current of electrons through an energy barrier is proportional to the tunneling probability of an electron through the barrier. In the WKB approximation, the tunneling probability of an electron at the Fermi level is

$$T = \exp\left[-2 \int_{(\text{barrier})} dz \sqrt{\frac{2m^*(E_c(z) - E_F)}{\hbar^2}}\right], \quad (2)$$

where $E_c(z)$ is the conduction band minimum (refer to FIG. 2). Because the energy barrier due to the spacer in a typical quantum wire is small ($l_s = 20$ nm and $E_{off} = 0.2$ eV typically), the corresponding tunneling current is so large that it keeps electrons on both sides in equilibrium no matter how the gate voltage changes. On the other hand, the barrier at the exposed surface is very high ($l_c = 10$ nm, $l_d = 40$ nm, and $\Phi_{sb} = 0.8$ eV typically), therefore the corresponding tunneling current is so small that the surface electrons are isolated and the total number of the surface electrons is conserved although the gate voltage

changes.

Feature 4) We assume that, after a quantum wire has been fabricated and no gate voltage is applied, the surface electrons share the same Fermi energy with the 2DEG. We also assume that this equilibrium also holds after the quantum wire undergoes illumination at the zero gate voltage.

This assumption is based on the consideration that the high-temperature ($T \sim 500$ K) fabrication process provides the conditions necessary for the whole system to reach equilibrium. That is, the surface electrons share the same Fermi energy with the rest of the system. After the quantum wire is illuminated, the surface electrons do not necessarily stay in equilibrium with the others. However, by assuming the equilibrium of the whole system after illumination, we have a starting point for calculation of the effect that an illumination has on the quantum wires. Moreover, we speculate that the real situation of quantum wires after an illumination by photons with energies larger than Φ_{sb} is not too far from an equilibrium state, and therefore the evaluated results should provide useful information.

Based on the four features presented above, we are able to set up the electrostatic formalism for any quantum wire system and make predictions. However, we need first to determine the shallow donor density N_s , which is not directly known from the sample fabrication conditions or from experimental measurements. We find that N_s can be determined from n_0 , the 2DEG density at the zero gate voltage, which can be obtained by extrapolating the densities measured from edge state backscattering experiments [41,42] to zero gate voltage. However, the relation between N_s and n_0 depends on the ionization regime of shallow donors in the doped $\text{Al}_x\text{Ga}_{1-x}\text{As}$ layer. Therefore, we need to analyze the ionization regimes of the doped layer at zero gate voltage.

B. Ionization Regimes

The ionization regimes here refer to the spatial arrangement of the ionized shallow donors in the doped layer, and to the way that the donated electrons are distributed between the

2DEG and the surface states, at zero gate voltage. For the quantum wire shown in FIG. 1, there are three ionization regimes.

In ionization regime A, the band bending is shown in FIG. 3a. In this regime, all of the shallow donors in the doped layer are ionized and no 2DEG is present. Because the bottom of the conduction band in the GaAs channel layer is higher than the surface (interface) levels, all donated electrons transfer to the $z = 0$ plane to fill the surface (interface) states. The electrons accumulated at the $z = 0$ plane in effect form a ‘capacitor’ with the positively ionized donors in the doped layer. Thus the conduction band in the GaAs channel layer is not affected by the transfer of electrons and remains flat. The ionization of the doped layer falls into this regime when the shallow donor density is very low.

In ionization regime B, the band bending is shown in FIG. 3b. In this regime, all the shallow donors in the doped layer are ionized and a 2DEG is formed at the $z = L$ plane. Note that the curved conduction band within the doped layer has a minimum point M which divides the whole doped layer into two parts, with thicknesses l_1 and l_2 , respectively. Because the electric field at M is zero, one may consider all of the donated electrons from the region to the left of M to transfer to the $z = 0$ plane thus form a ‘capacitor’, while all the donated electrons to the right of M transfer to the $z = L$ plane to form another ‘capacitor’. These two capacitors have no interaction each other because each screens itself completely. Such a consideration enables us to discuss each capacitor separately.

Ionization regime C is the most complicated and its band bending structure is shown in FIG. 2. Regime C differs from regime B by the presence of an *unionized region* in the doped layer. In the unionized region, the bound levels of shallow donors are not above the Fermi level, thus the electrons in this region are not ionized and remain bound to the donors. Correspondingly, the whole doped layer is divided into three parts. The left hand one forms one ‘capacitor’ with the surface (interface) electrons, the right hand one forms another ‘capacitor’ with the 2DEG, and the central one is charge neutral with its conduction band being flat. The ionization occurs in regime C when the shallow donor density is very high.

For the quantum wire shown in FIG. 1 with fixed geometric dimensions, as the shallow density increases, the ionization of the doped layer progresses from regime A to B, to C. In studying quantum wires, however, we are only interested in the ionization regimes B and C when the 2DEG is present. Usually the ionization is in regime B before illumination and in regime C after sufficient illumination, because the shallow donor density is increased by illumination.

To identify the ionization regime of a particular quantum wire at the zero gate voltage, we need to calculate the critical characteristic parameters. Notice that since the exposed surface Schottky barrier Φ_{sb} and the metal-GaAs contact Schottky barrier Φ'_{sb} may be quite different, we have to calculate the critical parameters under the gates and under the exposed surface separately. For under the exposed surface, let N_α be the critical shallow donor density that divides regimes A and B, and N_β be the one that divides regimes B and C. Under the gates, let N'_α and N'_β be the corresponding critical parameters.

Now let us calculate N_α and N_β . When $N_s = N_\alpha$, the bottom of conduction band in the GaAs channel layer (the region denoted ‘flat’ in FIG. 3a) lines up with the system’s Fermi level, and with the energy level of the surface states. Therefore,

$$\frac{e^2 N_\alpha}{\varepsilon \varepsilon_0} (l_c l_d + \frac{l_d^2}{2}) = \Phi_{sb}, \quad (3)$$

in which the left side gives the total band bending in the cap and the doped layers. The two band offsets at $z = l_c$ and $z = L$ cancel each other. (Here, as well as in following discussion, we take the ‘capacitor’ to be large and neglect its edge effects.)

When $N_s = N_\beta$, the minimum point M in FIG. 3b just touches the x-axis. That is, the bottom of the conduction band at M is at the system’s Fermi level. Therefore we have

$$\frac{e^2 N_\beta}{\varepsilon \varepsilon_0} (l_c l_1 + \frac{l_1^2}{2}) = \Phi_{sb} + E_{off}, \quad (4)$$

$$\frac{e^2 N_\beta}{\varepsilon \varepsilon_0} (l_s l_2 + \frac{l_2^2}{2}) = E_{off} - E_{z0}, \quad (5)$$

$$l_1 + l_2 = l_d, \quad (6)$$

where equations 4 and 5 come from the fact that the bottom of conduction band at point

M is equal to the Fermi energy of surface electrons and of the 2DEG.

Note that, in equation 5, E_{z0} is the energy difference between the 2DEG Fermi energy and the bottom of the conduction band at $z = L$, as shown in FIG. 3b. Typically $E_{z0} \sim 0.04$ eV but E_{z0} vanishes when electrons are nearly depleted. [3] Because E_{z0} is comparable to E_{off} , we include its effect in equation 5. (E_{z0} does not appear in equation 3, because electrons are depleted in that situation.)

When $N_s = N_\beta$, the corresponding density of surface electrons is

$$n_\beta^{sur} = N_\beta l_1, \quad (7)$$

and the density of the 2DEG is

$$n_\beta = N_\beta l_2, \quad (8)$$

where N_β , l_1 , and l_2 are obtained by solving equations 4, 5, and 6.

For the doped layer under the gates, the critical parameter values N'_α and N'_β can be calculated similarly except that the surface states are replaced by the interface states and Φ_{sb} by Φ'_{sb} .

We can identify the ionization regime of a particular quantum wire by comparing its actual shallow donor density N_s to its calculated critical values N_α and N_β . However, N_s , being a part of N_{total} , is usually not known directly. On the other hand, the 2DEG density n_0 at zero gate voltage can readily be determined experimentally. Therefore, it is more convenient to work in terms of the comparison between n_β and n_0 . The conditions for different ionization regimes of the doped layer *under the exposed surface* are listed in TABLE I. (The conditions for the ionization regimes of the doped layer *under the gates* are obtained by replacing N_α , N_β , and n_β in TABLE I by primed quantities.)

C. Determination of N_s

Now we evaluate N_s from the measured 2DEG density n_0 at zero gate voltage. For a quantum wire in ionization regime B, N_s is obtained by solving the following equations

$$\frac{e^2 N_s}{\varepsilon \varepsilon_0} (l_c l_1 + \frac{l_1^2}{2}) - \frac{e^2 N_s}{\varepsilon \varepsilon_0} (l_s l_2 + \frac{l_2^2}{2}) = \Phi_{sb} + E_{z0}, \quad (9)$$

$$l_1 + l_2 = l_d, \quad (10)$$

$$N_s l_2 = n_0, \quad (11)$$

where l_1 and l_2 have been shown in FIG. 3b. Equation 9 comes from the condition that the surface energy level is equal to that of the 2DEG.

If the ionization of the quantum wire is in regime C (see FIG. 2), then N_s should be calculated from

$$\frac{e^2 N_s}{\varepsilon \varepsilon_0} [l_s l_2 + \frac{l_2^2}{2}] = E_{off} - E_{z0}, \quad (12)$$

$$N_s l_2 = n_0, \quad (13)$$

where equation 12 comes from the Fermi level of the 2DEG being equal to the bound level of shallow donors in the unionized region.

D. Depletion Voltage

In a quantum wire, a 2DEG is usually present at the $z = L$ plane before any gate voltage is applied. When a negative gate voltage is applied to the gates, the density of the 2DEG is decreased. The depletion voltage $-V_{dep}$ is the gate voltage at which electrons of the 2DEG are completely depleted from under the gates. The depletion voltage is an important parameter because it characterizes the transition of the system of electrons at the $z = L$ plane from two-dimensional to quasi-one-dimensional.

The gate voltage actually measures the energy difference between the Fermi level in the gates and the Fermi level in the GaAs at $z = L$. Therefore, (noting that $E_{z0} = 0$ at depletion), the depletion voltage is given by

$$eV_{dep} = \frac{e^2 N_s}{\varepsilon \varepsilon_0} (l_c l_d + \frac{l_d^2}{2}) - \Phi'_{sb}, \quad (14)$$

where the first term on the right side gives the total band bending in the cap and the doped layers, and Φ'_{sb} is the Schottky barrier of the gate-GaAs contact. Note that N_s should

be determined from the measured 2DEG density n_0 according to the ionization regime at the zero gate voltage. From equation 14, the depletion voltage should be independent of illumination because N_s of the regions in the doped layer that are under the gates is not affected by illumination.

E. Pinchoff Voltage

The pinchoff voltage $-V_{pinch}$ is the gate voltage at which electrons are just completely depleted from the $z = L$ plane in the quantum wire. Therefore, it measures the energy difference between the Fermi level of electrons in the gates and the bottom of conduction band at the central point ($x = 0, z = L$) of the electron channel. The calculation of the pinchoff voltage is much more complicated than that of the depletion voltage, because it involves the electrostatic potential difference between at the point ($x = 0, z = L$) and the gates, and depends in an essential way on the fringing fields of the capacitors discussed in Section II B. The pinchoff voltage is affected by illumination because an illumination increases the shallow donor density under the exposed semiconductor surface and thus changes the charge distribution.

For the purpose of the calculation below, let the electrostatic potential just inside the semiconductor adjacent to the gates be zero and $-\varphi(x, z)$ be the potential function (noting that the system is y-independent). Then the pinchoff voltage is given by

$$eV_{pinch} = e\varphi(0, L) - \Phi'_{sb}, \quad (15)$$

where $e\varphi(0, L)$ is the potential energy at pinchoff of an electron at point ($x = 0, z = L$), and Φ'_{sb} is the gate-GaAs contact Schottky barrier.

The calculation of $-\varphi(0, L)$ can be done by using the Green's function method with the Dirichlet boundary condition. The general expression of the potential function for $z \geq 0$ contains two terms that correspond to the contributions from the spatial charge and from the boundary, respectively [44]

$$-\varphi(x, z) = -\varphi_1(x, z) + -\varphi_2(x, z) \quad (16)$$

$$= \frac{1}{4\pi\epsilon\epsilon_0} \iiint d^3r' \rho(\mathbf{r}') G(\mathbf{r}, \mathbf{r}') - \frac{1}{4\pi} \iint_{(z'=0)} dx' dy' \varphi(\mathbf{r}') \frac{\partial}{\partial z'} G(\mathbf{r}, \mathbf{r}'), \quad (17)$$

where $\mathbf{r} = (x, y, z)$, $\mathbf{r}' = (x', y', z')$, $\rho(\mathbf{r}')$ is the spatial charge density, and $G(\mathbf{r}, \mathbf{r}')$ is the Green's function, which is given by

$$\nabla'^2 G(\mathbf{r}, \mathbf{r}') = -4\pi\delta(\mathbf{r} - \mathbf{r}'), \quad (18)$$

$$G(\mathbf{r}, \mathbf{r}')|_{z'=0} = 0. \quad (19)$$

Using the image method, the solution of the Green's function is

$$G(\mathbf{r}, \mathbf{r}') = \frac{1}{[(x' - x)^2 + (y' - y)^2 + (z' - z)^2]^{1/2}} - \frac{1}{[(x' - x)^2 + (y' - y)^2 + (z' + z)^2]^{1/2}}. \quad (20)$$

At an arbitrary gate voltage prior to the pinchoff voltage, there are electrons present at the $z = L$ plane and there may exist an unionized region in the doped layer as shown in FIG. 2. Therefore, the spatial charge density $\rho(\mathbf{r}')$ is not known analytically, and $-\varphi(x, z)$ can only be calculated numerically. At the pinchoff voltage, however, no electrons are present at the $z = L$ plane and the shallow donors everywhere in the doped layer must be ionized. (If there were an unionized region, there would have to be electrons present at the $z = L$ plane because the bottom of the conduction band in the GaAs channel layer is lower than that in the doped layer by E_{off} .) Because of this, it is possible to calculate $-\varphi(x, z)$ analytically at the pinchoff voltage.

Because the shallow donors are all ionized, before illumination, the spatial charge density can be expressed as

$$\rho(\mathbf{r}) = \begin{cases} eN_s, & \text{if } l_c \leq z \leq l_c + l_d \\ 0, & \text{otherwise} \end{cases} \quad (21)$$

The contribution from the spatial charge, the first term on the right side of equation 17, can thus be calculated easily and the result is

$$-\varphi_1(x, z) = \frac{eN_s}{\varepsilon\varepsilon_0} \times \begin{cases} l_d z, & \text{if } z < l_c \\ -\frac{1}{2}(z - l_c - l_d)^2 + l_c l_d + \frac{1}{2}l_d^2, & \text{if } l_c \leq z \leq l_c + l_d \\ l_c l_d + \frac{1}{2}l_d^2, & \text{if } z > l_c + l_d \end{cases} \quad (22)$$

which is independent of x . For the central point ($x = 0, z = L$),

$$\varphi_1(0, L) = \frac{eN_s}{\varepsilon\varepsilon_0} (l_c l_d + \frac{l_d^2}{2}), \quad (23)$$

which gives the total band bending in the cap and the doped layers. (We have obtained this result previously in Section II B by using consideration of the capacitor.)

After an illumination, the spatial shallow donor density has been increased in the doped layer under the exposed surface (Feature 1). As an approximation, we can take the spatial charge density as

$$\rho(\mathbf{r}) = \begin{cases} eN_{sl}, & \text{if } x \leq |w| \text{ and } l_c \leq z \leq l_c + l_d \\ eN_s, & \text{if } x > |w| \text{ and } l_c \leq z \leq l_c + l_d \\ 0, & \text{otherwise} \end{cases} \quad (24)$$

in which $N_{sl} > N_s$ because the shallow donor density has been increased under the exposed surface. N_{sl} can be determined in the same way as N_s from the 2DEG density after illumination at zero gate voltage.

After performing the integration, the potential due to the spatial charge after illumination can be expressed as

$$\varphi_{1l}(0, L) = \varphi_1(0, L) [1 - \frac{N_{sl} - N_s}{N_{sl}} (\alpha_1 + \alpha_2)], \quad (25)$$

where $\varphi_1(0, L)$ is given by equation 23, and $\alpha_1 = L/\pi w$ and $\alpha_2 = -L^3/3\pi w^3$.

Now let us calculate the boundary contribution, the second term in equation 17. For split-gate quantum wires, we have a technical problem with potential value at the boundary potential ($z = 0$). Although we know the boundary potential near the gates (which has been chosen to be zero here), we do not know exactly how the boundary potential is distributed on the exposed surface. Strictly speaking, the potential distribution on the exposed surface

depends on the detailed information of the surface states. But the physics of surface states is very complicated and a calculation including the full details of the surface states is not feasible. However, in studying quantum wires, we find that it is sufficient to make some simple assumptions based on the properties of the surface states which have been described in Feature 3.

Considering the symmetry of quantum wires, the potential function at the exposed surface can be expanded as

$$-\varphi(x, 0) = \sum_{k=0}^{\infty} a_k x^{2k}, \quad |x| \leq w. \quad (26)$$

where $\{a_k\}$ are constant coefficients. We find it necessary to keep the first two terms in the expansion 26. Such a treatment makes it possible to ensure that the surface potential is continuous at $x = \pm w$. This yields

$$-\varphi(x, 0) = \begin{cases} V_0(1 - x^2/w^2), & \text{if } |x| \leq w \\ 0, & \text{if } |x| > w \end{cases} \quad (27)$$

where V_0 is a constant and will be determined later. Substituting equation 27 into the second term in equation 17, the boundary contribution is

$$-\varphi_2(x, z) = \frac{V_0}{\pi w^2} [(w^2 + z^2 - x^2)\theta(x, z) + xz \ln \frac{(w+x)^2 + z^2}{(w-x)^2 + z^2} - 2wz], \quad (28)$$

where

$$\theta(x, z) = \arctan \frac{w-x}{z} + \arctan \frac{w+x}{z}, \quad (29)$$

which is just the angle that is subtended by the exposed surface at the point (x, z) . Therefore,

$$e\varphi_2(0, L) = \frac{2eV_0}{\pi} \left[\left(1 + \frac{L^2}{w^2}\right) \arctan \frac{w}{L} - \frac{L}{w} \right]. \quad (30)$$

The boundary contribution $-\varphi_2(x, z)$ actually describes the potential that laterally confines the electrons at the $z = L$ plane. To help visualize this confining potential, we plot $e\varphi_2(x, z)$ in $z > 0$ half space in FIG. 4. The intersection of the plot with the $z = L$ plane

just gives the confining potential well profile. The larger L is, the more shallow the potential well becomes.

Now V_0 can be determined by the conservation of the total number of surface electrons (Feature 3). That is

$$\int_{-w}^w n^{sur}(x)dx = 2ewN_sl_1, \quad (31)$$

in which the right side expresses the linear charge density of the exposed surface at zero gate voltage, and the left side is the linear charge density at the pinchoff voltage. The area surface density is evaluated based on the calculated $-\varphi(x, z)$, to yield

$$en^{sur}(x) = \frac{2\varepsilon\varepsilon_0V_0w}{\pi w^2} \left[x \ln \frac{(w+x)^2}{(w-x)^2} - 4w \right] - eN_sl_d. \quad (32)$$

Finally, we discuss briefly the relationship between the work presented in this section and the earlier work of Davies [19] who was the first to study the boundary contribution to the potential of a quantum wire using the Green's function method. Davies considered only the leading term in the expansion 26 of the surface potential. However, for our purposes this approximation is not adequate since it yields a discontinuous potential along the surface instead of equation 27, and as a consequence, a surface charge density for which the integral in equation 31 diverges. By retaining also the second term of the expansion 26, we obtain a continuous surface potential and a finite integrated surface charge density 32. This enables us to use the conservation of the surface charge at the exposed surface to evaluate the parameter V_0 .

III. DISCUSSION OF A REAL SAMPLE

Now let us take a real split-gate quantum wire as an example for calculating the depletion and pinchoff voltages using the present theory.

The sample quantum wire we consider has the typical structure displayed in FIG. 1. Grown with MBE on a semi-insulating GaAs substrate, its layers in sequence are a 65 nm

GaAs buffer, 30 periods of GaAs/AlAs superlattice, 900 nm GaAs channel layer, 1.5 nm AlAs and 16 nm undoped $\text{Al}_{0.33}\text{Ga}_{0.67}\text{As}$ layers as the spacer, 40 nm Si-doped $\text{Al}_{0.33}\text{Ga}_{0.67}\text{As}$ layer with donor concentration of $1.1 \times 10^{18} \text{ cm}^{-3}$, and 18 nm GaAs cap layer with normal surface (100). On top of the GaAs cap, two separated gate bars of titanium are applied using electron beam lithography. The gate bars have a spatial separation of 200 nm and width of 200 nm.

Analysis after growth shows that the undoped $\text{Al}_{0.33}\text{Ga}_{0.67}\text{As}$ layer of the spacer is 14.5 nm instead of the expected value 16 nm. This suggests that all of the actual thicknesses should be reduced by 10% from their expected values. Correspondingly, the concentration of the Si donors in the doped $\text{Al}_{0.33}\text{Ga}_{0.67}\text{As}$ layer should be increased by 10% so as to keep the nominal total number of donors. The parameter values that we use in our calculations are listed in TABLE II.

According to equations 3, 4, 5, 6, and 8, the calculated critical values that separate the ionization regimes of this sample are $N_\alpha = 0.45 \times 10^{18} \text{ cm}^{-3}$, $N_\beta = 0.80 \times 10^{18} \text{ cm}^{-3}$, and $n_\beta = 6.03 \times 10^{11} \text{ cm}^{-2}$.

Now let us consider three situations of the quantum wire: before illumination, after one illumination, and after many illuminations (i.e. after saturation with a red light emitting diode). Corresponding to these three situations, the measured densities of the 2DEG at zero gate voltage are $3.40 \times 10^{11} \text{ cm}^{-2}$, $5.49 \times 10^{11} \text{ cm}^{-2}$, and $6.25 \times 10^{11} \text{ cm}^{-2}$, respectively. Comparing these measured values to the calculated critical value $n_\beta = 6.03 \times 10^{11} \text{ cm}^{-2}$ and referring to TABLE II, the ionization regimes of this quantum wire before illumination, after one illumination, and after many illuminations are in B, B, and C, respectively. The corresponding shallow donor densities and the depletion voltage and pinchoff voltages can therefore be calculated based on the formalism in Section II. The calculated results are presented in TABLE III.

Experimentally, the depletion and pinchoff voltages can be known from the measured longitudinal (y-direction) resistances against the gate voltage. [47,48] The measured resistance curves of the sample quantum wire are displayed in FIG. 5. Curves a, b, and c

correspond to the resistances varying with the gate voltage before illumination, after one illumination, and after many illuminations, respectively. The depletion voltages for curves a, b, and c are -0.33 V, -0.35 V and -0.37 V, respectively, which agree very well with the calculated results -0.33 V. (The negative increases of depletion voltage upon illumination can be explained by the fact that the gate bars are very narrow and therefore some illuminating photons may penetrate into the regions under the gates and excite the deep donor there.) The pinchoff voltages read from curves a, b, and c are about -0.55 V, -0.86 V, and -1.33 V, respectively, which are fairly close to their corresponding calculated results -0.53 V, -0.80 V, and -1.43 V.

In conclusion, this paper presents an electrostatic model of split-gate quantum wires and sets up a general formalism that is applicable both before and after illumination. For any split-gate quantum wire, given its geometric parameters and its measured 2DEG density at zero gate voltage, additional information such as its ionization state, shallow donor density, depletion voltage, and pinchoff voltage can be calculated based on the model. While contributing to our understanding of the electrostatic characteristics of quantum wires, this model suggests a potential approach for studying the electrodynamic and time-dependent processes in quantum wires. The theory of this paper should also provide a tool for study other gated nanostructures such as multiple constrictions [49–52] and quantum dots [53–55].

We would like to acknowledge helpful discussions with C. J. B. Ford, MBE material grown by P. T. Coleridge and fabrication assistance from P. Chow-Chong, M. Davies, P. Marshall, R. P. Taylor, and R. Barber. This work was supported by the Natural Sciences and Engineering Research Council of Canada and the Centre for Systems Science at Simon Fraser University.

REFERENCES

- [1] L. L. Chang and B. C. Giessen, in *Synthetic Modulated Structures* (Academic, Orlando, 1985); J. D. Grange, “The Growth of the MBE III-V Compounds and Alloys”, in *The Technology of Molecular Beam Epitaxy*, edited by E. H. C. Parker (Plenum Press, New York, 1992).
- [2] R. Dingle et al., Appl. Phys. Lett. **7**, 665 (1978).
- [3] For a review, see J. Harris, J. A. Pals, and R. Woltjer, Rep. Prog. Phys. **52**, 1217 (1989).
- [4] R. G. Wheeler, K. K. Choi, A. Goel, R. Wisnieff, and D. E. Prober, Phys. Rev. Lett. **49**, 1674 (1982).
- [5] A. Scherer, M. L. Roukes, H. G. Craighead, R. M. Ruthen, E. D. Beebe, and J. P. Harbison, Appl. Phys. Lett. **51**, 2133 (1987).
- [6] Y. Hirayama, S. Tarucha, Y. Suzuki, and H. Okamoto, Phys. Rev. **37**, 2774 (1988).
- [7] A. D. Wieck and K. Ploog, Appl. Phys. Lett. **56**, 928 (1990).
- [8] W. J. Skocpol, L. D. Jackel, E. L. Hu, R. E. Howard, and L. A. Fetter, Phys. Rev. Lett. **49**, 951 (1982).
- [9] J. P. Kirtley et. al., Phys. Rev. **B34**, 5414 (1986).
- [10] H. van Houten, B. J. van wees, M. G. J. Heijman, and J. P. André, Appl. Phys. Lett. **49**, 1781 (1986).
- [11] T. J. Thornton, M. Pepper, H. Ahmed, D. Andrews, and G. J. Davies, Phys. Rev. Lett. **56**, 1198 (1986).
- [12] H. Z. Zhang, H. P. Wei, D. C. Tsui, and G. Weimann, Phys. Rev. **B34**, 5635 (1986).
- [13] For a recent review see S. E. Ulloa, A. MacKinnon, E. Castaño, and G. Kirczenow, “From Ballistic Transport to Localization”, in *Handbook of Semiconductors* Vol. I, edited

- by P. T. Landsberg (North-Holland, Amsterdam, 1992).
- [14] F. W. Sheard and L. Eaves, *Nature* **333**, 600 (1988).
 - [15] A. Khurana, *Physics Today* **41**, 21 (1988).
 - [16] W. Y. Lai and S. Das Sarma, *Phys. Rev.* **B33**, 8874 (1986).
 - [17] S. E. Laux and F. Stern, *Appl. Phys. Lett.* **49**, 91 (1986).
 - [18] S. E. Laux, D. J. Franck, and F. Stern, *Surf. Sci.* **196**, 101 (1988).
 - [19] J. H. Davies, *Semicond. Sci. Technol.* **3**, 995 (1988).
 - [20] J. A. Nixon and J. H. Davies, *Phys. Rev.* **B 41**, 7929 (1990).
 - [21] A. Nakamura and A. Okiji, *J. Phys. Soc. Jpn.* **60**, 1873 (1991).
 - [22] U. Ravaioli, T. Kerkhoven, M. Raschke, and A. T. Galick, *Superlatt. Microstruc.* **11**, 343 (1992).
 - [23] Y. Sun and G. Kirczenow, *Phys. Rev.* **B47**, 4413 (1993); Y. Sun and G. Kirczenow, *Phys. Rev. Lett.* **72**, 2450 (1994)
 - [24] W. Kohn, *Solid State Phys.* **5** 257 (1957).
 - [25] N. Lifshitz, A. Jayaraman, and R. A. Logan, *Phys. Rev.* **B 21**, 670 (1980).
 - [26] T. Ishikawa, J. Saito, S. Sasa, and S. Hiyamizu, *Jpn. J. Appl. Phys.* **21**, L675 (1982).
 - [27] N. Chand, T. Henderson, J. Klem, W. T. Masselink, R. Fischer, Y. C. Chang, and H. Morkoc, *Phys. Rev.* **B 80**, 4431 (1984).
 - [28] D. V. Lang, “DX Centers in III-V Alloys”, in *Deep Centers in Semiconductors*, edited by S. T. Pantelides (Gordon and Breach Science Publishers, Switzerland, 1992).
 - [29] K. J. Malloy and K. Khchaturyan, “DX and Related Defects in Semiconductors”, *Semiconductors and Semimetals* Vol. 38, edited by E. R. Weber (Academic Press, San Diego,

- 1993).
- [30] D. V. Lang and R. A. Logan, Phys. Rev. Lett. **39**, 635 (1977).
 - [31] See, for examples, W. Mönch, *Semiconductor Surfaces and Interfaces* (Springer-Verlag, Berlin, 1993).
 - [32] J. R. Waldrop, J. Vac. Sci. Technol. **B 2**, 445 (1984).
 - [33] N. Newman, W. E. Spicer, T. Kendelewicz, and I. Lindau, J. Vac. Sci. Technol. **B 4**, 931 (1986).
 - [34] A. B. McLean, D. A. Evans, and R. H. Williams, Semicond. Sci. Technol. **2**, 547 (1986);
A. B. McLean and R. H. Williams, J. Phys. C **21**, 783 (1988).
 - [35] For a review see W. E. Spicer, I. Lindau, P. Skeath, and C. Y. Su, J. Vac. Sci. Technol. **17**, 1019 (1980).
 - [36] T.-C. Chiang, R. Ludeke, M. Aono, G. Landgren, F. J. Himpsel, D. E. Eastman, **B 27**, 4770 (1983).
 - [37] W. Pötz and D. K. Ferry, Phys. Rev. **B 31**, 968 (1985).
 - [38] R. P. Beres, R. E. Allen, and J. D. Dow, Solid State Commun. **45**, 13 (1983).
 - [39] C. B. Duke, “Tunneling in Solids”, in *Solid State Physics*, Supplement Vol. 10, edited by F. Seitz, D. Turnbull, and H. Ehrenreich (Academic Press, New York, 1969).
 - [40] G. Garcia-Calderón, “Tunneling in Semiconductor Resonant Structures”, in *Physics of Low-Dimensional Semiconductor Structures*, edited by P. Butcher, N. H. March, and M. P. Tosi (Plenum Press, New York, 1993).
 - [41] R. J. Haug, A. H. MacDonald, P. S. Treda, and K. von Klitzing Phys. Rev. Lett. **61**, 2797 (1988).
 - [42] S. Washburn, A. B. Fowler, H. Schmid, and D. Kern, Phys. Rev. Lett. **61**, 2801 (1988).

- [43] Experimentally, the bulk density of the 2DEG can be determined by Shubnikov de Haas measurements.
- [44] See for example J. D. Jackson, *Classical Electrodynamics*, 2nd Edition (John Wiley & Sons, New York, 1975), Section 1.10.
- [45] Keeping more terms in the expansion will modify the calculated distribution of the surface charge density. However, such a change (for fixed total surface charge) has no significant effect on the potential at the $z = L$ plane because this plane is far away from the surface.
- [46] H. Okumura, S. Misawa, S. Yoshida, and S. Gonda, Appl. Phys. Lett. **46**, 377 (1985).
- [47] B. J. van Wees, H. van Houten, C. W. J. Beenakker, J. G. Williamson, L. P. Kouwenhoven, D. van der Marel, and C. T. Foxon, Phys. Rev. Lett. **60**, 848 (1988).
- [48] D. A. Wharam, T. J. Thornton, R. Newbury, M. Pepper, H. Ahmed, J. E. F. Frost, D. G. Hasko, D. C. Peacock, D. A. Ritchie, and G. A. C. Jones, J. Phys. C: Solid State Phys. **21**, L209 (1988).
- [49] C. G. Smith, M. Pepper, R. Newbury, H. Ahmed, D. G. Hasko, D. C. Peacock, J. E. F. Frost, D. A. Ritchie, G. A. C. Jones, and G. Hill, J. Phys.: Condens. Matter **1**, 6763 (1989).
- [50] S. W. Hwang, J. A. Simmons, D. C. Tsui, and M. Shayegan, Phys. Rev. **44**, 13497 (1991).
- [51] P. E. Schmit, M. Okada, K. Kosemura, and N. Yokoyama, Jpn. J. Appl. Phys. **30**, L1921 (1991).
- [52] P. J. Simpson, D. R. Mace, C. J. B. Ford, I. Zailer, M. Pepper, D. A. Ritchie, J. E. F. Frost, G. A. C. Jones, Appl. Phys. Lett. **63**, 3191 (1993).
- [53] M. A. Reed et al., Phys. Rev. Lett. **60**, 535 (1988).

- [54] L. P. Kouvenhoven et al., Phys. Rev. Lett. **65**, 535 (1990).
- [55] A. Lorke, J. P. Kotthaus, and K ploog, Phys. Rev. Lett. **64**, 2559 (1990).

FIGURES

FIG. 1. Crossection of a typical split-gate quantum wire and the coordinate frame chosen for calculations.

FIG. 2. A possible band bending structure within quantum wires. The curve shows the bottom of the conduction band along the z -axis. E_{off} is the band offset at the interfaces between GaAs and $\text{Al}_x\text{Ga}_{1-x}\text{As}$.

FIG. 3. Band bending structures for ionization regime A (a) and ionization regime B (b), see text.

FIG. 4. A Three-dimensional representation of the potential energy $e\varphi_2(x, z)$ due to the boundary contribution for $z \geq 0$. Used parameters are $w = 100$ (nm) and $V_0 = 1$ (arbitrary unit).

FIG. 5. The measured resistances of the sample quantum wire. Curves a, b, and c are for the cases of the wire before illumination, after one illumination, and after many illuminations, respectively.

TABLES

TABLE I. Criteria for identifying different ionization regimes of the doped layer under the exposed surface in quantum wires at zero gate voltage.

Ionization regime	By shallow donor density N_s	By 2DEG density n_0
A	$N_s < N_\alpha$	$n_0 = 0$
B	$N_\alpha < N_s < N_\beta$	$0 < n_0 < n_\beta$
C	$N_s > N_\beta$	$n_0 > n_\beta$

TABLE II. Parameters used in calculations for the real sample of quantum wire

Description	Notation	Value	Unit
gate separation	$2w$	200	nm
GaAs cap layer	l_c	16.2	nm
doped Al _{0.33} Ga _{0.67} As layer	l_d	36	nm
Al _{0.33} Ga _{0.67} As and AlAs spacer	l_s	15.75	nm
effective mass	m^*	0.067	m_e
dielectric constant of GaAs	ϵ	12.5	
Schottky barrier of GaAs surface (100) [36]	Φ_{sb}	0.80	eV
Schottky barrier of Ti-GaAs contact [32]	Φ'_{sb}	0.83	eV
band offset [46]	E_{off}	0.2	eV
z-direction energy interval [3]	E_{z0}	0.04	eV

TABLE III. Calculated results of the real quantum wire

Parameter	Before ill.	After one ill.	After many ill.	Unit
Ionization regime	B	B	C	
measured 2DEG density n_0	3.40	5.49	6.25	10^{11} cm^{-2}
shallow donor density	0.65	0.77	1.02	10^{18} cm^{-3}
l_1	30.89	28.87	24.03	nm
l_2	5.11	7.13	6.11	nm
l_3	0	0	5.86	nm
calculated $-V_{dep}$	-0.33	-0.33	-0.33	V
calculated $-V_{pinch}$	-0.53	-0.80	-1.43	V

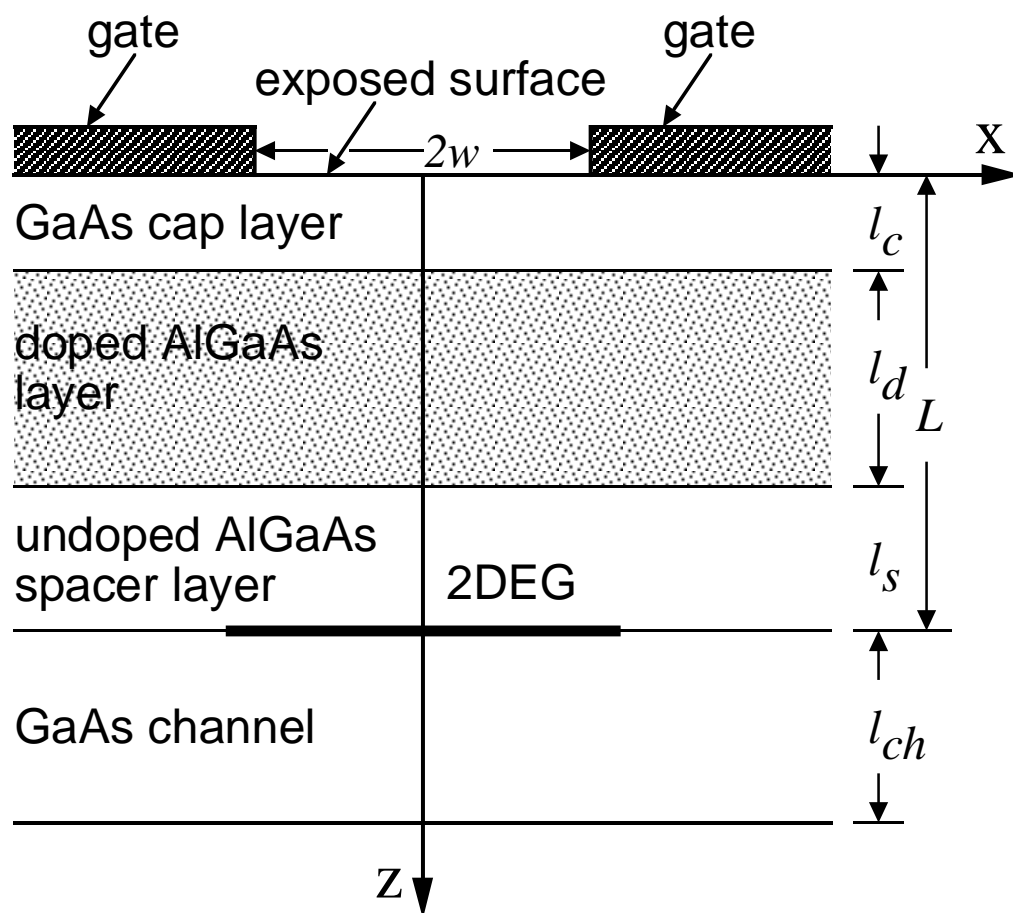


Figure 1

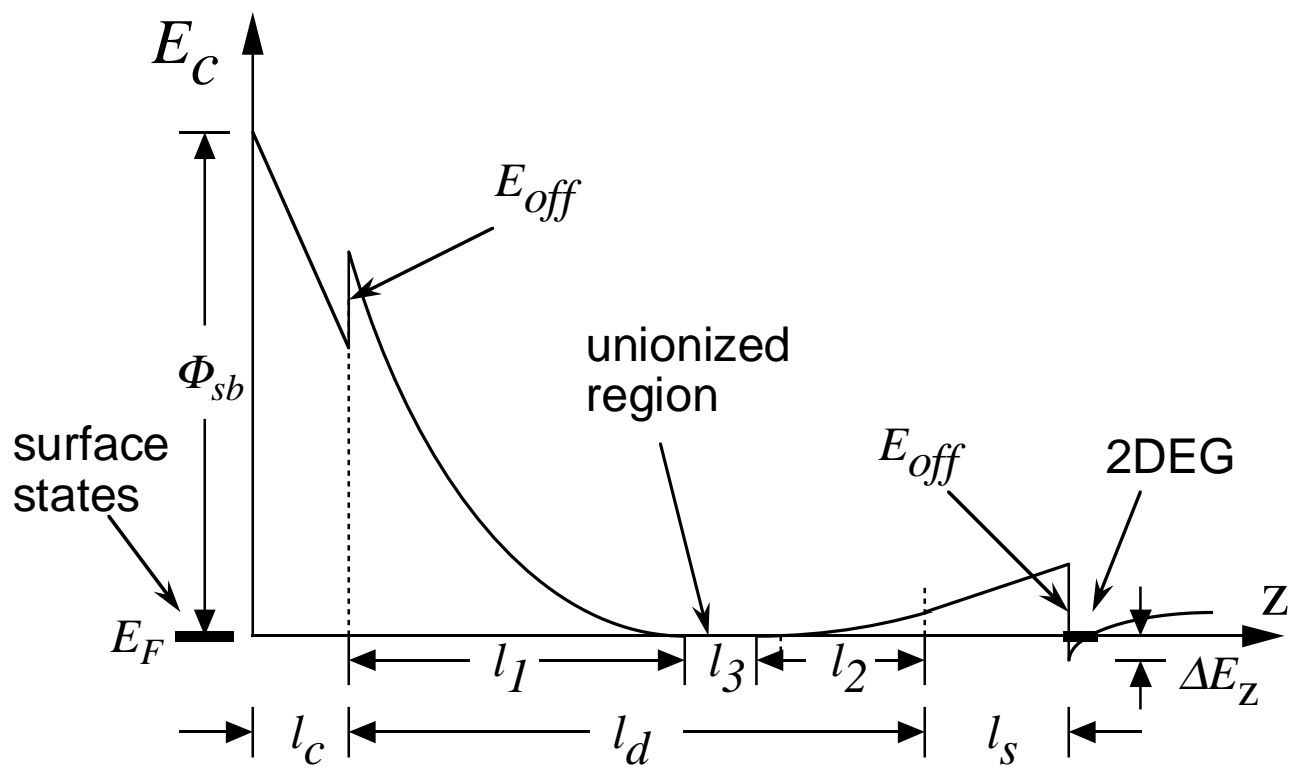


Figure 2

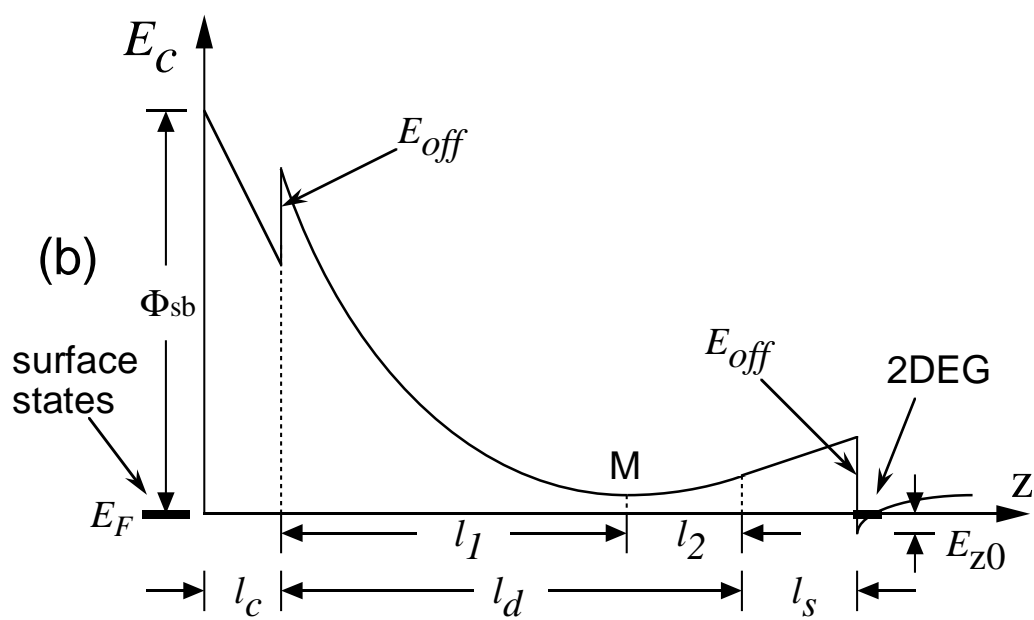
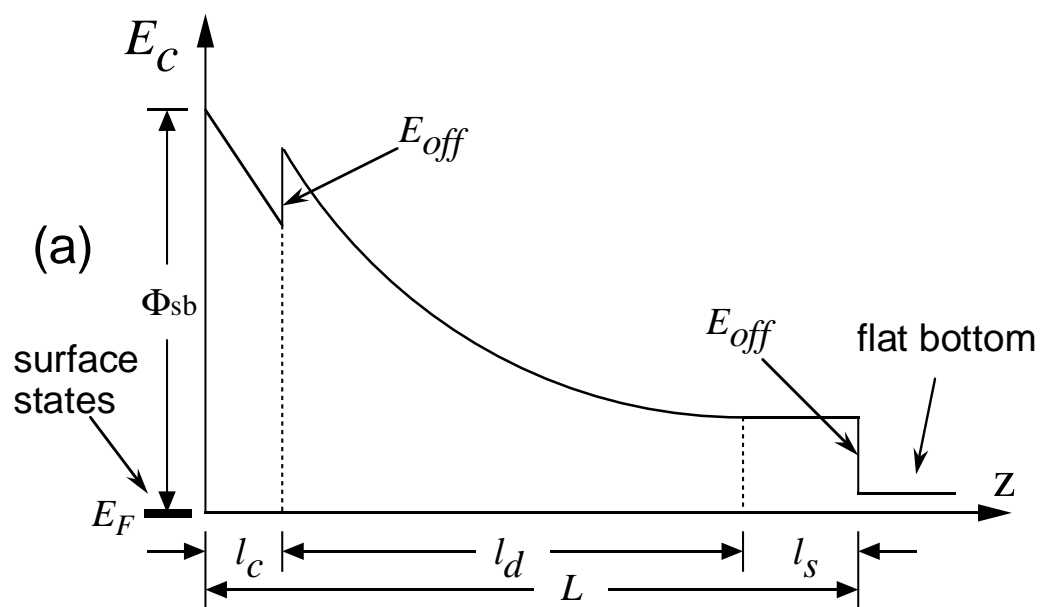


Figure 3

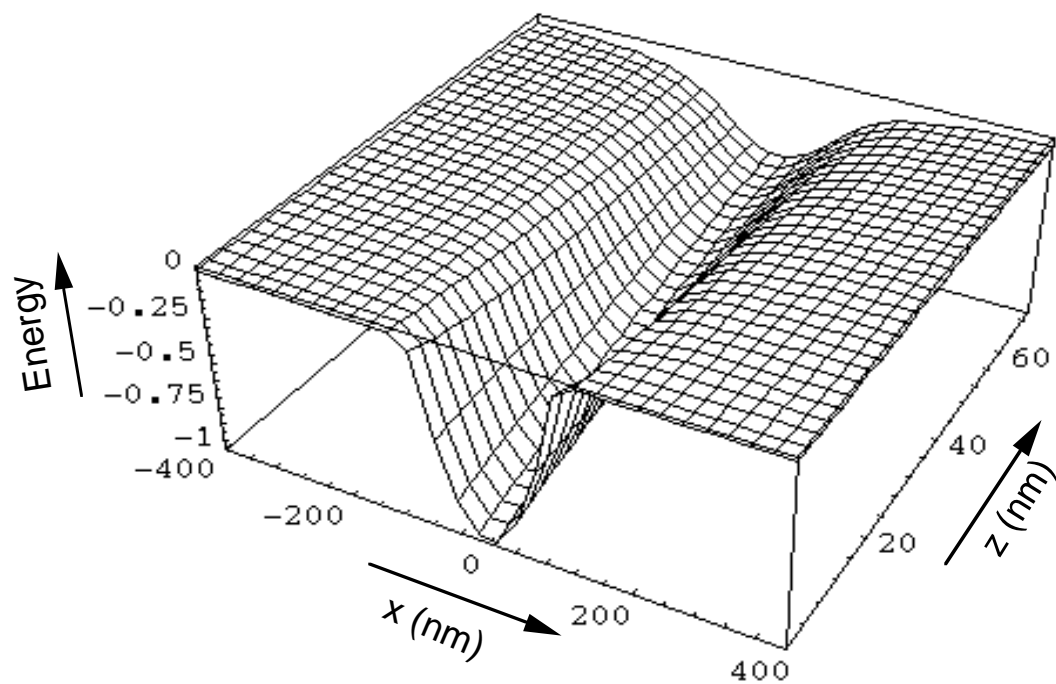


Figure 4

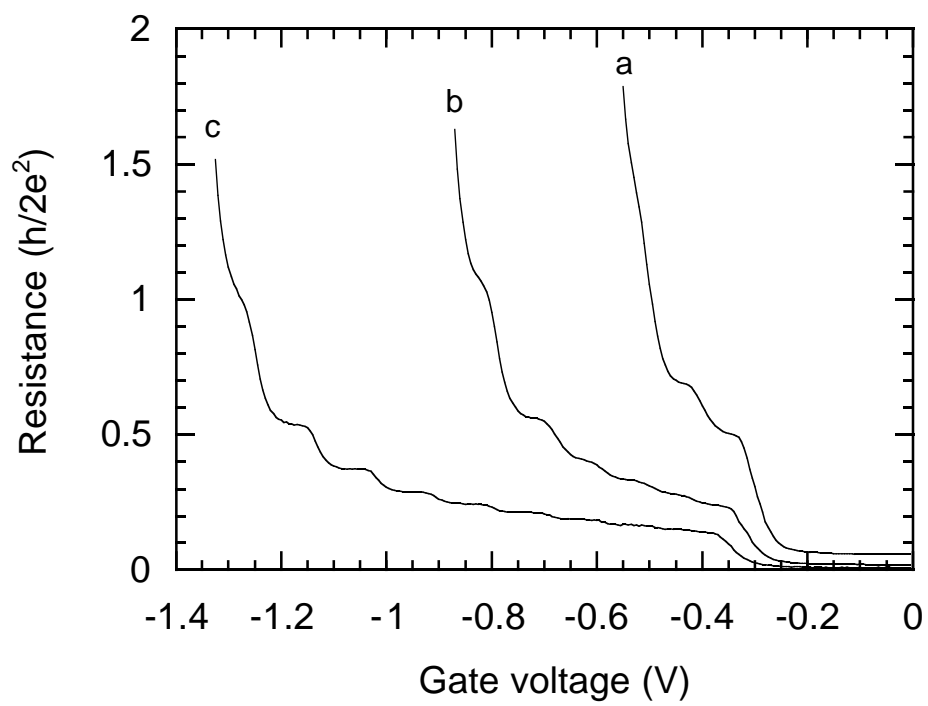


Figure 5